Stretching Response of a Polymer Chain with Deformable Bonds

Jie Zhu and Laurence Brassart*
Department of Engineering Science, University of Oxford, Oxford OX1 3PJ, United Kingdom

(Received 13 February 2025; revised 7 April 2025; accepted 30 April 2025; published 28 May 2025)

The stretching response of polymer chains fundamentally determines the mechanical properties of polymer networks. In this Letter, we develop a statistical mechanics model that incorporates both bond stretching and bond angle deformation, enabling accurate predictions of chain behavior up to large forces. We further propose a semianalytical deformable freely rotating chain (dFRC) model, which represents the chain as a freely rotating chain with effective bond stretch and bond angle that depend on the chain stretch. Using physical parameters without fitting, both the statistical and dFRC models achieve excellent agreement with experimental data for carbon chains across all force regimes. Additionally, the dFRC model provides a direct estimate of the bond force, which is important to predict chain scission. By capturing key bond deformations while remaining computationally efficient, our work lays the foundation for future modeling of polymer network elasticity and failure.

DOI: 10.1103/PhysRevLett.134.218101

The molecular structure and conformations of polymer chains fundamentally determine the macroscopic mechanical properties of polymer networks. Accordingly, chain models serve as key building blocks for polymer network studies, including mean-field theories [1–3], discrete network models [4–6], and continuum mechanics models [7–9]. When a polymer network is subjected to large deformations, such as during fracture, cavitation, or rapid loading, some chains can become highly stretched and eventually rupture. In these situations, the chain behavior is dominated by energetic contributions due to bond stretching and bond angle opening [10–12]. Therefore, single chain models that are valid up to large stretches are needed.

Classical entropic chain models, such as the freely jointed chain (FJC) and freely rotating chain (FRC) models [13], do not account for energetic contributions and thus cannot capture the high-force behavior. On the other hand, the wormlike chain (WLC) model is commonly adopted to account for bending energy in semiflexible polymers [14] but is limited to small equilibrium bond angles. Although extendable FJC and WLC models have been proposed [15–24], they do not simultaneously accommodate both bond stretching and bond angle opening with a finite equilibrium bond angle, raising concerns about the physical meaning of their best-fit parameters and their relevance to chain scission.

*Contact author: laurence.brassart@eng.ox.ac.uk

In this Letter, we address this limitation by developing a statistical mechanics model and a semianalytical model that explicitly incorporate both bond stretching and bond angle deformation in the stretching behavior of polymer chains. In the statistical model, we use the transfer-matrix (TM) technique to calculate the partition function in the Gibbs ensemble, from which we obtain the Gibbs free energy and force-extension relationship. Our results show that both bond stretching and bond angle opening significantly affect the chain stiffness at high forces. Using the TM calculations as reference, we further develop a semianalytical model by representing the polymer chain as a deformable FRC (dFRC) where the bond length and bond angle depend on the applied chain stretch, inspiring from original ideas in Refs. [20,25]. This is achieved by developing a new explicit formula for the classical FRC, which is shown to be valid across the entire force range. Using molecular mechanics-derived parameters without any fitting, both the statistical and dFRC models accurately predict the force-extension behavior of carbon chains and exhibit excellent agreement with experimental data over all force regimes. By capturing key bond-level deformations while maintaining computational efficiency, the dFRC model provides a foundation for advancing polymer network modeling, particularly in scenarios involving failure by chain scission, where bond force predictions are important.

We consider a polymer chain composed of N bonds (Fig. 1). The conformation of the chain is described by the positions $\vec{r}_i$ of each atom $(i = 0, \ldots, N)$. The chain is subjected to a prescribed force $\vec{f}$ at the terminal atom $\vec{r}_N$, with the other terminal atom fixed at the origin $\vec{r}_0 = (0, 0, 0)$. Each bond vector, $\vec{l}_i = \vec{r}_i - \vec{r}_{i-1}$, $(i = 1, \ldots, N)$, is represented in spherical coordinates as

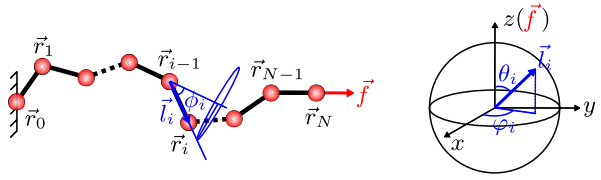

FIG. 1. A polymer chain with N bonds subjected to a constant force $\vec{f}$ at $\vec{r}_N$. The other chain end at $\vec{r}_0$ is fixed. The orientation of each bond is described using spherical coordinates, with the z axis aligned with the force.

$\vec{l}_i = l_i(\sin\theta_i\cos\varphi_i, \sin\theta_i\sin\varphi_i, \cos\theta_i)$, where l_i is the bond length, θ_i is the polar angle relative to the direction of the applied force $\vec{f}$, and φ_i is the azimuthal angle. The bond angle between adjacent bonds, $\phi_i = \angle(\vec{l}_{i-1}, \vec{l}_i)$, $(i = 2, \ldots, N)$, is calculated as $\phi_i = \arccos[\sin\theta_i\sin\theta_{i-1}\cos\omega_i + \cos\theta_i\cos\theta_{i-1}]$, where $\omega_i = \varphi_i - \varphi_{i-1}$ is the difference in azimuthal angle between two adjacent bonds.

The partition function for the chain in the Gibbs ensemble is given by (Supplemental Material, Sec. S1 [26]):

$$Z \propto \int e^{-\frac{1}{k_BT}\left[\sum_{i=1}^{N} v_{\mathrm{str}}(l_i) + \sum_{i=2}^{N} v_{\mathrm{ben}}(\phi_i) - \sum_{i=1}^{N} f l_i \cos\theta_i\right]} dq, \quad (1)$$

where $q = (\vec{l}_1, \ldots, \vec{l}_N)$, k_B is the Boltzmann constant, T is the temperature, and $f = \|\vec{f}\|$. The bond stretching energy is assumed quadratic for simplicity: $v_{\mathrm{str}}(l_i) = \frac{1}{2}k_l(l_i - l_e)^2$, where l_e is the equilibrium bond length, and k_l is the bond stretching stiffness. Similarly, the bond angle deformation energy ("bending energy") is taken as $v_{\mathrm{ben}}(\phi_i) = \frac{1}{2}k_\phi(\phi_i - \phi_e)^2$, where ϕ_e is the equilibrium bond angle, and k_ϕ is the bond bending stiffness. We neglect the bond rotation energy, as it is typically much smaller than the energies associated with bond stretching and bending in homogeneous backbone chains (e.g., carbon-carbon backbone) [11], so that bonds can freely rotate. In addition, we neglect the long-range interactions between atoms that are far apart along the chain contour, so that the chain is an ideal chain [13].

The bending energy couples the configurations of two consecutive bonds. Consequently, the Gibbs partition function [Eq. (1)] cannot be factorized into N identical terms, different from the extensible FJC model. To address this difficulty, we employ the numerical TM method [31,32], building on the work of Livadaru *et al.*, who applied this technique to the FRC model [33]. The weighted probability density of finding the $(i+1)$th bond at an angle θ can be expressed as (Supplemental Material, Sec. S2.1 [26]):

$$W_{i+1}(\theta) = \int P_i(\theta')T(\theta, \theta')d\theta', \quad (2)$$

where $P_i(\theta) = W_i(\theta)/[\int W_i(\theta')d\theta']$ is the bond orientation probability density of the i th bond, and $\int P_i(\theta)d\theta = 1$. The transfer operator $T(\theta, \theta')$ characterizes the interaction between the $(i+1)$ th bond at angle θ and the i th bond at angle θ', which is given by

$$T(\theta, \theta') = \iint e^{-\frac{1}{k_BT}[v_{\mathrm{str}}(l) + v_{\mathrm{ben}}(\phi) - fl\cos\theta]} l^2 \sin\theta d\omega dl, \quad (3)$$

where l is the length of the $(i+1)$ th bond, ϕ is the bond angle between the $(i+1)$ th and i th bonds, and ω is the difference in their azimuthal angles. The weighted probability density of the first bond is given by

$$W_1(\theta) = \iint e^{-\frac{1}{k_BT}[v_{\mathrm{str}}(l) - fl\cos\theta]} l^2 \sin\theta d\omega dl, \quad (4)$$

where ω is the azimuthal angle of the first bond. Starting with $W_1(\theta)$, the weighted probability density of each subsequent bond can be determined iteratively. Finally, the Gibbs partition function [Eq. (1)] can be obtained as (Supplemental Material, Sec. S2.1 [26])

$$Z \propto \prod_{i=1}^{N}\left[\int W_i(\theta)d\theta\right]. \quad (5)$$

The chain end-to-end distance r is derived from the Gibbs partition function as

$$r = k_BT\frac{\partial}{\partial f}\ln Z = -\frac{\partial G}{\partial f}, \quad (6)$$

where $G = -k_BT\ln Z$ is the Gibbs free energy. Note that $r = \|\vec{r}\| = \|\langle\vec{r}_N\rangle\|$ is the norm of the ensemble average of the chain end-to-end vector. The partition function is calculated using quadrature methods, and the force-extension relationship is obtained by numerical differentiation (Supplemental Material, Sec. S2.1 [26]). The special cases of freely jointed bonds ($k_\phi = 0$) and fixed bond angles ($k_\phi \to \infty$) are discussed in Supplemental Material, Secs. S2.2 and S2.3, respectively. Bond orientation probability densities $P_i(\theta)$ are illustrated in Sec. S3, where we show that $P_i(\theta)$ converges to a stable distribution $P_\infty(\theta)$ as the bond index i increases. For sufficiently large N, the Gibbs partition function [Eq. (5)] can be approximated as $Z \propto [\int W_\infty(\theta)d\theta]^N$, where $W_\infty(\theta) = \int P_\infty(\theta')T(\theta, \theta')d\theta'$ is the converged weighted probability density. The resulting force-extension relationship becomes independent of N, corresponding to the thermodynamic limit. The effect of N on the force-extension relationship is further discussed in Supplemental Material, Sec. S4.1.

We examine how bond stretching and bond angle opening influence the stretching response in the thermodynamic limit ($N \to \infty$). To isolate their individual effects, we analyze the following limiting cases: (i) Freely jointed

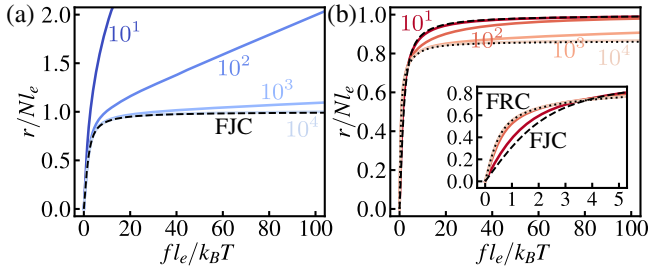

FIG. 2. Effect of bond deformation on the stretching response of polymer chains. (a) Chains with freely jointed extensible bonds ($k_\phi = 0$; $k_l l_e^2/k_BT = 10^1, 10^2, 10^3, 10^4$). (b) Chains with rigid bonds ($k_l l_e^2/k_BT \to \infty$) and deformable bond angles ($\phi_e = 60°$; $k_\phi \pi^2/k_BT = 10^1, 10^2, 10^3, 10^4$).

extensible bonds. Force-extension curves are shown in Fig. 2(a) for different values of the normalized bond stretching stiffness, $k_l l_e^2/k_BT$. At low forces, the chain stretching response is primarily governed by entropic elasticity and follows the Gaussian chain model $r = Nl_e^2 f/(3k_BT)$, where $Nl_e^2/(3k_BT)$ represents the entropic spring constant [13]. As the force increases, bond stretching results in a second elastic regime with chain stiffness proportional to k_l. In the limit $k_l l_e^2/k_BT \to \infty$, the extensible FJC model recovers the FJC model with contour length $R_{\max} = Nl_e$. These results are consistent with the findings in Ref. [16].

(ii) Rigid bonds and deformable bond angles. Force-extension curves are shown in Fig. 2(b) for $\phi_e = 60°$ and different values of the normalized bond bending stiffness, $k_\phi \pi^2/k_BT$. For $k_\phi = 0$, the model recovers the FJC model. For $k_\phi \pi^2/k_BT \to \infty$, the model tends to the FRC model with contour length $R_{\max} = Nl_e \cos(\phi_e/2)$. At low applied forces, increasing k_ϕ softens the chain since the coiled configuration becomes less probable. As the force increases, a larger k_ϕ stiffens the chain as it approaches its extensibility limit. This stiffening effect depends on the equilibrium bond angle ϕ_e, with a larger ϕ_e leading to a reduced contour length, see Supplemental Material, Sec. S4.2 [26].

While the statistical model effectively captures the effect of bond deformation on the stretching response of polymer chains, its lack of a closed-form expression limits practical use in single-molecule experiments and polymer network modeling. To address this, we further develop a semi-analytical approximation. Following the approach proposed by Lavoie *et al.* [25], we assume uniform and nonfluctuating bond length l and bond angle ϕ. The Helmholtz free energy Ψ of a polymer chain under a prescribed end-to-end distance r is then given by

$$\Psi = N v_{\text{str}}(l) + (N-1) v_{\text{ben}}(\phi) + \Psi_{\text{ent}}(r, l, \phi), \quad (7)$$

where the first two terms, respectively, represent the energetic contributions due to bond stretching and bond angle deformation, and the third term Ψ_{ent} is the entropic contribution. In Ref. [25], Ψ_{ent} was obtained by integrating the closed-form force-extension relation of the WLC model, where the persistence length was expressed in terms of l and ϕ. However, this WLC representation introduces additional approximations which are difficult to quantify. Here, in contrast, we directly take Ψ_{ent} as the free energy of a FRC with bond length l and bond angle ϕ, consistent with the decomposition in Eq. (7). The bond parameters l and ϕ are determined by minimizing the Helmholtz free energy at a prescribed chain end-to-end distance r, which implies $(\partial\Psi/\partial l)_{r,\phi} = (\partial\Psi/\partial\phi)_{r,l} = 0$. The force-displacement response is then derived as $f = d\Psi/dr = (\partial\Psi_{\text{ent}}/\partial r)_{l,\phi}$. We refer to this model as the "deformable FRC" (dFRC).

The practical implementation of the dFRC model requires an explicit expression for the force-extension relationship of the FRC, valid across the entire force range. However, existing formulations are either limited to specific force ranges or implicit [10,33]. To address this, we propose a new explicit formula for the FRC, guided by its limiting behaviors at small and large deformations (Supplemental Material, Sec. S5 [26]):

$$f = \frac{k_BT}{l_k}\left\{\beta + \frac{1}{2}\frac{(r^*)^2}{(1-r^*)^2}\left[1 - (r^*)^{l_k/l-1}\right]\right\}, \quad (8)$$

where $\beta = \mathcal{L}^{-1}(r^*)$ and $\mathcal{L}(x) = \coth(x) - 1/x$ is the Langevin function. Here, $r^* = r/R_{\max}$ represents the relative end-to-end distance, with the contour length given by $R_{\max} = Nl\cos(\phi/2)$. The equivalent Kuhn length is $l_k = \langle r^2\rangle/R_{\max} = 2l\cos(\phi/2)/(1-\cos\phi)$, where the mean-square end-to-end distance is $\langle r^2\rangle = Nl^2(1+\cos\phi)/(1-\cos\phi)$ [13]. Equation (8) shows a remarkable agreement with TM calculations across a wide range of bond angles ($\phi = 10° - 90°$), maintaining a relative error below 6% over the entire force range ($fl_e/k_BT = 10^{-3.5} - 10^{2.5}$) (Supplemental Material, Fig. S10 [26]). The FRC free energy $\Psi_{\text{ent}}(r, l, \phi)$ is obtained by integrating the force-extension relation as $\Psi_{\text{ent}}(r, l, \phi) = \int f dr$, giving

$$\Psi_{\text{ent}} = k_BT\frac{R_{\max}}{l_k}\left[r^*\beta + \ln\frac{\beta}{\sinh\beta} + \frac{1 + r^*(1-r^*)}{2(1-r^*)} + \ln(1-r^*) - \frac{1}{2}\mathcal{B}(r^*; 2 + l_k/l, -1)\right], \quad (9)$$

where $\mathcal{B}(x; a, b) = \int_0^x t^{a-1}(1-t)^{b-1}dt$ is the incomplete beta function. For freely jointed bonds ($k_\phi = 0$), only bond stretching is considered, with the bond length l determined by energy minimization. In this case, the Kuhn length and contour length are $l_k = l$ and $R_{\max} = Nl$, respectively. The force-extension relationship [Eq. (8)] recovers the FJC model with $f = (k_BT/l_k)\beta$, and the entropic energy [Eq. (9)] becomes $\Psi_{\text{ent}}(r, l) = Nk_BT[r^*\beta + \ln(\beta/\sinh\beta)]$.

This recovers the semianalytical extensible FJC model, see Ref. [20].

We validate the semianalytical dFRC model for a polymer chain with extensible bonds and deformable bond angles by comparing its predicted force-extension relationships to reference predictions from the statistical model (TM calculations). Additionally, we assess the model core assumptions of uniform and nonfluctuating bond length and bond angle by analyzing corresponding probability densities obtained from TM calculations (Supplemental Material, Sec. S6 [26]). The semianalytical extensible FJC model is similarly validated against the statistical model in Supplemental Material, Sec. S6.1. Here, we consider two representative cases: (i) Extensible bonds and fixed bond angles. In the statistical model, the bond length probability density $P_i^l(l)$ depends on the bond index i but quickly converges to $P_\infty^l(l)$ as i increases (Supplemental Material, Fig. S13 [26]), supporting the uniform bond length assumption. This converged distribution depends on the bond stretching stiffness k_l, which controls the length variance, and the applied force f, which shifts the average bond length (Supplemental Material, Fig. S14 [26]). As shown in Fig. 3(b), for $k_l l_e^2/k_BT = 10^3$, $P_\infty^l(l)$ remains concentrated around its most probable value, supporting the nonfluctuating bond length assumption. The optimized bond length in the dFRC model closely follows the peak of $P_\infty^l(l)$, yielding an accurate force-extension prediction [Fig. 3(a)]. Even for $k_l l_e^2/k_BT = 10^1$, where the bond length is more widely distributed, the dFRC model still approximates the force-extension response well (Supplemental Material, Fig. S15 [26]).

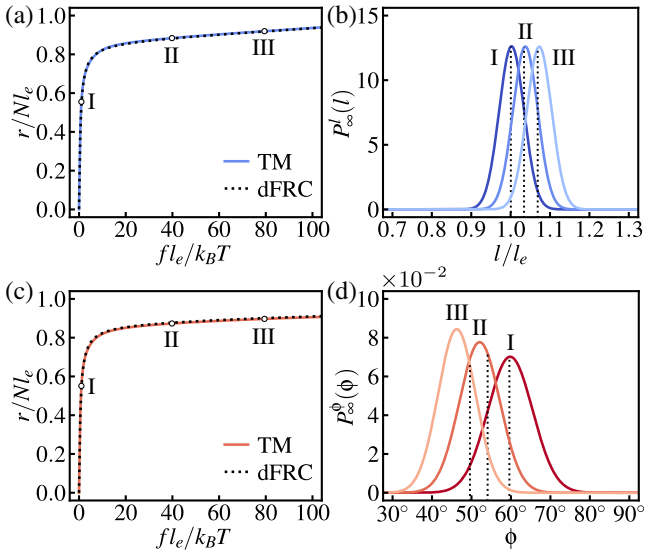

FIG. 3. Comparison of statistical (TM) and dFRC models for chains with deformable bonds. (a) Force-extension curves for a chain with extensible bonds ($k_l l_e^2/k_BT = 10^3$) and fixed bond angles ($k_\phi \pi^2/k_BT \to \infty$, $\phi_e = 60°$). (b) Converged bond length distribution in the statistical model at different forces from (a). (c) Force-extension curves for a chain with rigid bonds ($k_l l_e^2/k_BT \to \infty$) and deformable bond angles ($k_\phi \pi^2/k_BT = 10^3$, $\phi_e = 60°$). (d) Corresponding converged bond angle distribution from (c). In (b) and (d), black dotted lines indicate the optimized bond lengths or angles in the dFRC model.

(ii) Rigid bonds and deformable bond angles. With increasing bond index i, the bond angle probability density $P_i^\phi(\phi)$ given by the statistical model quickly converges to $P_\infty^\phi(\phi)$ (Supplemental Material, Fig. S17 [26]), supporting the uniform bond angle assumption. This converged distribution depends on the bond bending stiffness k_ϕ and the applied force f (Supplemental Material, Fig. S18 [26]). For $k_\phi \pi^2/k_BT = 10^3$, $P_\infty^\phi(\phi)$ is narrowly distributed, supporting the nonfluctuating bond angle assumption [Fig. 3(d)]. As f increases, $P_\infty^\phi(\phi)$ narrows further and shifts to the left, indicating a reduction in both the average and variability of the bond angles. At lower forces, the optimized bond angle in the dFRC model aligns closely with the peak of $P_\infty^\phi(\phi)$, corresponding to the most probable bond angle. However, at higher forces, the optimized value overestimates the most probable value [Fig. 3(d)]. Nevertheless, the dFRC model still accurately predicts the force-extension relation [Fig. 3(c)]. The accuracy of the dFRC model also depends on k_ϕ. As k_ϕ decreases, the bond angle distribution broadens, and the dFRC model performance deteriorates, becoming inapplicable for $k_\phi \pi^2/k_BT = 10$ (Supplemental Material, Fig. S19 [26]).

Finally, we apply our statistical and dFRC models to polymer chains with a carbon-carbon backbone, such as polyethylene, polystyrene, and polypropylene. Molecular mechanics calculations indicate that these chains have an equilibrium bond length of $l_e = 1.53$ Å and an equilibrium bond angle of $\phi_e = 69°$, with bond stiffness $k_l = 4.29 \times 10^{-18}$ J/Å^2 for stretching and $k_\phi = 7.47 \times 10^{-19}$ J/rad^2 for bending [34]. Using these parameters, we simulate chain stretching at room temperature ($T = 23°$) and compare predictions with experimental data from [11]. For reference, we also include the equivalent FJC model (FJC*), which represents the chain using rigid Kuhn segments of length $l_k = 2l_e \cos(\phi_e/2)/(1 - \cos\phi_e)$, and the FRC model, which considers rigid bonds of length l_e and fixed bond angles at ϕ_e. As shown in Fig. 4(a), all models agree well with experimental data at small deformations ($r/R_0 \leq 0.8$), where the response is entropy dominated. Here, $R_0 = Nl_e \cos(\phi_e/2)$ is the contour length at zero force. At intermediate forces ($0.8 < r/R_0 \leq 0.9$), the FRC model outperforms the FJC* model by incorporating fixed bond angles, thereby better capturing the effect of angular constraints on chain conformations. However, at large deformations ($r/R_0 > 0.9$), the FRC model diverges from experimental data as bond deformations become significant. Additional comparisons with extensible FJC* and FRC models reveal that using physical

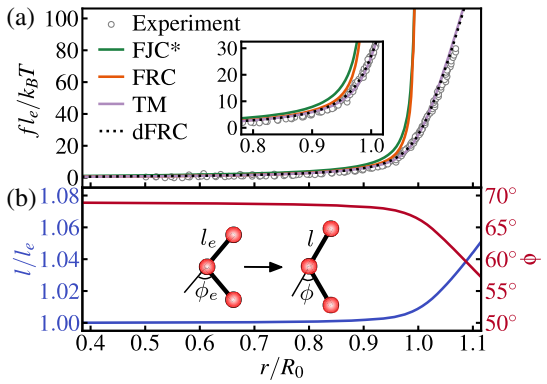

FIG. 4. Stretching response of carbon chains. (a) Comparison of predictions from the FJC*, FRC, statistical (TM) and dFRC models against experimental data from [11]. (b) Evolution of bond length l and bond angle ϕ in the dFRC model. R_0 denotes the contour length at zero force.

parameters alone fails to capture the large deformation response (Supplemental Material, Sec. S7 [26]). This highlights the necessity of incorporating both bond stretching and bond angle opening in chain elasticity models. In contrast, our statistical (TM) and dFRC models remain accurate across the entire force range by capturing these energetic effects [Fig. 4(a)]. Both bond stretching and bond angle opening contribute significantly to the response, as indicated by the dimensionless bond parameters $k_l l_e^2/k_BT = 2466$ and $k_\phi \pi^2/k_BT = 1810$, which strongly influence chain stiffness at high forces (Fig. 2). These parameters also ensure the close agreement between the dFRC and statistical models (Fig. 3).

Beyond improving chain-level force-extension predictions, the dFRC model also provides access to internal bond-level variables. As shown in Fig. 4(b), it predicts the evolution of bond length and bond angle with increasing chain extension. For extension ratios $r/R_0 \leq 0.9$, the response is entropy dominated, with bond lengths and angles close to their equilibrium values. Consequently, the force-extension curve in this regime aligns with the FRC model [Fig. 4(a)]. At larger extensions, energetic contributions become significant, leading to bond stretching and bond angle opening. Based on the predicted bond length, the bond force can be obtained as $f_b = \partial v_{\mathrm{str}}(l)/\partial l = k_l(l - l_e)$. In the entropy-dominated regime, f_b remains nearly zero due to negligible bond stretching, but it increases as deformation progresses, potentially leading to bond breakage and chain scission [25,35–38].

In summary, we have presented two complementary models that accurately capture the stretching behavior of polymer chains up to large deformations by incorporating both bond stretching and bond angle opening simultaneously. Without relying on parameter fitting, both models show excellent agreement with experimental data on carbon chain stretching across all force regimes. The semianalytical dFRC model, in particular, balances accuracy with computational efficiency and provides bond-level resolution, making it suitable for integration into polymer network simulations aimed at predicting elasticity and failure. While we adopted quadratic forms for bond stretching and bending energies, our framework is not restricted to these choices and can accommodate more general potentials, such as Lennard-Jones or Morse potentials. It can also be extended to hybrid chains with multiple backbone bond types or less flexible chains with large side groups and strong rotation hindrance. Overall, this work provides a robust foundation for advancing physically grounded and predictive modeling of polymer network mechanics, particularly under extreme deformation and failure conditions.

Acknowledgments—The authors thank Lucas Mangas Araujo from University of Oxford and Kangjie Zheng from Peking University for important discussions and helpful comments on the manuscript. J. Z. acknowledges the support of an EPSRC DTP studentship at the University of Oxford. L. B. acknowledges support from UKRI through a Future Leaders Fellowship [MR/W006995/1].

Data availability—The data that support the findings of this article are openly available [39].

[1] H. M. James, Statistical properties of networks of flexible chains, J. Chem. Phys. **15**, 651 (1947).
[2] C. Storm, J. J. Pastore, F. C. MacKintosh, T. C. Lubensky, and P. A. Janmey, Nonlinear elasticity in biological gels, Nature (London) **435**, 191 (2005).
[3] S. Feng, M. F. Thorpe, and E. Garboczi, Effective-medium theory of percolation on central-force elastic networks, Phys. Rev. B **31**, 276 (1985).
[4] A. A. Gusev, Numerical estimates of the topological effects in the elasticity of Gaussian polymer networks and their exact theoretical description, Macromolecules **52**, 3244 (2019).
[5] G. Alamé and L. Brassart, Effect of topological defects on the elasticity of near-ideal polymer networks, J. Appl. Mech. **87**, 121006 (2020).
[6] L. M. Araujo, I. Kryven, and L. Brassart, Micromechanical modelling of rubbery networks: The role of chain pre-stretch, Int. J. Nonlinear Mech. **166**, 104834 (2024).
[7] M. C. Boyce and E. M. Arruda, Constitutive models of rubber elasticity: A review, Rubber Chem. Technol. **73**, 504 (2000).
[8] F. J. Vernerey, R. Long, and R. Brighenti, A statistically-based continuum theory for polymers with transient networks, J. Mech. Phys. Solids **107**, 1 (2017).
[9] J. Mulderrig, B. Li, and N. Bouklas, Affine and non-affine microsphere models for chain scission in polydisperse elastomer networks, Mech. Mater. **160**, 103857 (2021).
[10] T. Hugel, M. Rief, M. Seitz, H. E. Gaub, and R. R. Netz, Highly stretched single polymers: Atomic-force-microscope experiments versus ab-initio theory, Phys. Rev. Lett. **94**, 048301 (2005).

[11] K. Wang, X. Pang, and S. Cui, Inherent stretching elasticity of a single polymer chain with a carbon–carbon backbone, Langmuir **29**, 4315 (2013).
[12] S. Lu, W. Cai, N. Cao, H. Qian, Z. Lu, and S. Cui, Understanding the extraordinary flexibility of polydimethylsiloxane through single-molecule mechanics, ACS Mater. Lett. **4**, 329 (2022).
[13] M. Rubinstein and R. H. Colby, *Polymer Physics* (Oxford University Press, New York, 2003).
[14] J. F. Marko and E. D. Siggia, Stretching DNA, Macromolecules **28**, 8759 (1995).
[15] N. Balabaev and T. Khazanovich, Extension of chains composed of freely joined elastic segments, Russ. J. Phys. Chem. B **3**, 242 (2009).
[16] F. Manca, S. Giordano, P. L. Palla, R. Zucca, F. Cleri, and L. Colombo, Elasticity of flexible and semiflexible polymers with extensible bonds in the Gibbs and Helmholtz ensembles, J. Chem. Phys. **136** (2012).
[17] A. Fiasconaro and F. Falo, Analytical results of the extensible freely jointed chain model, Physica (Amsterdam) **532A**, 121929 (2019).
[18] M. R. Buche, M. N. Silberstein, and S. J. Grutzik, Freely jointed chain models with extensible links, Phys. Rev. E **106**, 024502 (2022).
[19] J. Mulderrig, B. Talamini, and N. Bouklas, A statistical mechanics framework for polymer chain scission, based on the concepts of distorted bond potential and asymptotic matching, J. Mech. Phys. Solids **174**, 105244 (2023).
[20] Y. Mao, B. Talamini, and L. Anand, Rupture of polymers by chain scission, Extreme Mech. Lett. **13**, 17 (2017).
[21] A. Fiasconaro and F. Falo, Elastic traits of the extensible discrete wormlike chain model, Phys. Rev. E **107**, 024501 (2023).
[22] R. R. Netz, Strongly stretched semiflexible extensible polyelectrolytes and DNA, Macromolecules **34**, 7522 (2001).
[23] J. Kierfeld, O. Niamploy, V. Sa-Yakanit, and R. Lipowsky, Stretching of semiflexible polymers with elastic bonds, Eur. Phys. J. E **14**, 17 (2004).
[24] A. Rosa, T. Hoang, D. Marenduzzo, and A. Maritan, Elasticity of semiflexible polymers with and without self-interactions, Macromolecules **36**, 10095 (2003).
[25] S. R. Lavoie, R. Long, and T. Tang, Modeling the mechanics of polymer chains with deformable and active bonds, J. Phys. Chem. B **124**, 253 (2019).
[26] See Supplemental Material at http://link.aps.org/supplemental/10.1103/PhysRevLett.134.218101 for detailed analytical derivation, numerical implementation, parameter study, and model validation. Also refer Supplemental Material for derivation and application of the semi-analytical extensible FJC model, which includes Refs. [9,20,27–30].
[27] B. Talamini, Y. Mao, and L. Anand, Progressive damage and rupture in polymers, J. Mech. Phys. Solids **111**, 434 (2018).
[28] B. Li and N. Bouklas, A variational phase-field model for brittle fracture in polydisperse elastomer networks, Int. J. Solids Struct. **182**, 193 (2020).
[29] P. K. Arunachala, S. A. Vajari, M. Neuner, and C. Linder, A multiscale phase field fracture approach based on the non-affine microsphere model for rubber-like materials, Comput. Methods Appl. Mech. Eng. **410**, 115982 (2023).
[30] P. K. Arunachala, S. Abrari Vajari, M. Neuner, J. S. Sim, R. Zhao, and C. Linder, A multiscale anisotropic polymer network model coupled with phase field fracture, Int. J. Numer. Methods Eng. **125**, e7488 (2024).
[31] R. J. Baxter, *Exactly Solved Models in Statistical Mechanics* (Elsevier, New York, 2016).
[32] S. M. Ross, *Introduction to Probability Models* (Academic Press, New York, 2014).
[33] L. Livadaru, R. Netz, and H. Kreuzer, Stretching response of discrete semiflexible polymers, Macromolecules **36**, 3732 (2003).
[34] R. Sorensen, W. Liau, L. Kesner, and R. Boyd, Prediction of polymer crystal structures and properties: Polyethylene and poly (oxymethylene), Macromolecules **21**, 200 (1988).
[35] M. Grandbois, M. Beyer, M. Rief, H. Clausen-Schaumann, and H. E. Gaub, How strong is a covalent bond?, Science **283**, 1727 (1999).
[36] A. Ghatak, K. Vorvolakos, H. She, D. L. Malotky, and M. K. Chaudhury, Interfacial rate processes in adhesion and friction, J. Phys. Chem. B **104**, 4018 (2000).
[37] M. K. Chaudhury, Rate-dependent fracture at adhesive interface, J. Phys. Chem. B **103**, 6562 (1999).
[38] Q. Guo and F. Zaïri, A micromechanics-based model for deformation-induced damage and failure in elastomeric media, Int. J. Plast. **140**, 102976 (2021).
[39] J. Zhu and L. Brassart, SingleChainModels (Version 1.0), GitHub, 2025, https://github.com/JieZhu617/SingleChainModels.